

Article

Whole-Genome Identification and Expression Profiles of WRKY Genes Related to the Leaf Expansion Period in the Camphor tree

Shilin Long, Jingyao Jiang and Hanyang Lin *

Zhejiang Provincial Key Laboratory of Plant Evolutionary Ecology and Conservation, School of Life Sciences, Taizhou University, Taizhou 318000, China; 2263190034@stu.tzc.edu.cn (S.L.); 2231210014@stu.tzc.edu.cn (J.J.)

* Correspondence: hylin@tzc.edu.cn

Abstract: The camphor tree (*Cinnamomum camphora*) is of great economic and ecological value, and the WRKY transcription factor (TF) family plays a crucial role in regulating plant growth and development as well as the responses toward environmental changes. However, the research on WRKY TFs in *C. camphora* remains scarce, and their roles in the leaf expansion period are unknown. In this study, we identified WRKY TFs across the *C. camphora* genome, followed by a phylogenetic analysis. Then, we conducted RNA sequencing and qPCR experiments on leaves collected from three distinct stages during leaf expansion (S1, S2, and S3) to determine which WRKY genes showed significant up-regulation during these stages. Here, a total of 72 CcWRKY TFs were found in the *C. camphora* genome, and they were phylogenetically clustered with corresponding subfamilies of *Arabidopsis thaliana*. These CcWRKY proteins were divided into three major groups (I, II, and III), where group II consisted of five subgroups. We found that three genes (*CcWRKY24*, *CcWRKY42*, and *CcWRKY70*) were upregulated from both S1 to S2 and from S1 to S3. The expression level of *CcWRKY24* increased gradually from S1 to S3, while *CcWRKY42* and *CcWRKY70* exhibited higher expression levels in S2 and S3 than in S1. These predicted gene expression profiles were further confirmed by qPCR experiments. In summary, this study analyzed WRKY TFs in *C. camphora* from a genome-wide perspective and paves the way for future research on the functions of CcWRKYs.

Keywords: *Cinnamomum camphora*; WRKY transcription factor; phylogenetic analysis; gene expression; leaf expansion; RNA sequencing

Academic Editor: C. Dana Nelson

Received: 9 December 2024

Revised: 28 January 2025

Accepted: 1 February 2025

Published: 2 February 2025

Citation: Long, S.; Jiang, J.; Lin, H. Whole-Genome Identification and Expression Profiles of WRKY Genes Related to the Leaf Expansion Period in the Camphor tree. *Forests* **2025**, *16*, 266. <https://doi.org/10.3390/f16020266>

Copyright: © 2025 by the authors. Licensee MDPI, Basel, Switzerland. This article is an open access article distributed under the terms and conditions of the Creative Commons Attribution (CC BY) license (<https://creativecommons.org/licenses/by/4.0/>).

1. Introduction

WRKY is a key transcription factor (TF) mainly found in plants. The first WRKY TF was isolated from the sweet potato (*Ipomoea batatas*) by Ishiguro and Nakamura [1]. Since then, as research on the WRKY gene family has continued to deepen, many WRKY TFs have been identified in various plants, including thale cress (*Arabidopsis thaliana*), rice (*Oryza sativa*), and wheat (*Triticum aestivum*), among many others [2,3]. The WRKY TF name was derived from the seven conserved amino acids, namely WRKYGQK [4,5]. Traditionally, WRKY TFs can be classified into three groups (groups I, II, and III) based on the number of WRKY domains and the zinc finger types. The group I WRKY proteins contain two WRKY domains, while the other two WRKY groups are composed of one WRKY domain, but the zinc finger motif is different between the two WRKY groups [4]. Meanwhile, group II can be further divided into five subgroups (IIa, IIb, IIc, IId, and IIe). Nevertheless, phylogenetic analyses showed that group II domains designated by Eulgem et al. [4] were not monophyletic but formed three distinct clades instead (IIa + IIb, IIc, and IId + IIe) [6]. Among these groups, group IIc was close to group I while group III was clustered with group IId + IIe.

A body of research indicates that many WRKY TFs are involved in plant growth, development, senescence, and response to environmental changes [2,4,5,7–9]. For instance, numerous studies have confirmed that WRKY TFs are involved in the regulation of seed size (*A. thaliana* and soybean) [10,11], pollen development (*A. thaliana*) [12], flowering time (soybean) [13], fruit development (pepper and black wolfberry) [14,15], leaf senescence (*A. thaliana* and the Chinese flowering cabbage) [16–18], and petal senescence (the wallflower and tulips) [19,20]. Meanwhile, the WRKY TFs are involved in the responses to high temperature and drought stress (rice, birchleaf pear, and wheat) [21–23] and ion stress (wheat) [24]. WRKY TFs were extensively studied in *A. thaliana*. For example, previous studies have demonstrated that AtWRKY44 (also known as TTG2) controls the epidermal color of *A. thaliana* seeds by regulating vacuolar transport steps in the proanthocyanidin biosynthesis pathway [25]. Also, the overexpression of AtWRKY57 can increase the drought tolerance of *A. thaliana* [26]. Expression levels of AtWRKY4/6/7 and 11 would be enhanced in senescent leaves [4]. The AtWRKY12 and AtWRKY13 TFs control the flowering time of *A. thaliana* through the gibberellin signaling pathway and the functions of these two TFs differ in this process. For example, the knockout of the AtWRKY12 gene can delay the flowering time, while the loss of the AtWRKY13 function would promote the flowering process [27,28]. In short, WRKY TFs are crucial to numerous plant functions.

The camphor tree (*Cinnamomum camphora* (L.) J. Presl), a member of the Lauraceae family, is renowned for its rich aromatic oils and versatile values in multiple aspects, including ornamental, economic, ecological, and evolutionary ones [29–34]. Its attractive foliage and fragrance make it a popular ornamental plant [30]. In China, it starts rapid leaf expansion from April to May, during which its floral organs start to develop simultaneously [35]. Economically, the camphor tree is a significant industrial tree species globally, as it provides excellent wood for furniture making and sculpture crafting [29,30]. Meanwhile, its roots, stems, leaves, and fruits are abundant in essential oils and are widely utilized in cosmetics, food additives, insect repellents, and traditional Chinese herbal medicine [29,36,37]. Moreover, the camphor tree plays a critical role in the ecological benefits of forest ecosystems due to its considerable height, with some individuals reaching up to 40 meters [38,39]. For instance, it can fix a substantial amount of CO₂, effectively regulating local climate and improving soil quality, thereby playing a crucial role in both carbon fixation and mitigating global climate change [34,39]. Beyond its inherent values, the camphor tree is also a well-known fast-growing species for afforestation, significantly contributing to greening efforts worldwide [40]. Furthermore, the camphor tree has a vast distribution, with extensive distributions throughout major tropical and subtropical regions, as well as the transition zone between subtropical and temperate climates. This not only emphasizes its immense ecological significance but also showcases its remarkable adaptability to diverse environments [34,39].

In summary, *C. camphora* is of great economic and ecological value and provides us with an ideal material to study plant adaptation. Notwithstanding the importance of WRKY TFs and the camphor tree, previous works have mainly focused on the TPS, MYB, or NAC TF families, leaving the WRKY TFs relatively understudied [34,41–43] and poorly understood. Nevertheless, some preliminary results shed light on the importance of WRKY TFs in several biological processes in *C. camphora*. For example, Yang et al. (2021) [41] found that several WRKY genes interacted with TPS genes to participate in borneol biosynthesis. More recently, Li et al. (2023) [34] determined that some WRKY TFs were involved in triglyceride biosynthesis and circadian rhythm. Nevertheless, we still lack a comprehensive understanding of the distribution of WRKY TFs across the genome of *C. camphora* and their roles in response to changing environments (such as increasing temperatures) or in the regulation during individual development (such as the leaf expansion period), leading to an evident knowledge gap that calls for deeper investigations.

In the present study, we conducted a genome-wide analysis of CcWRKY TFs to determine their physicochemical properties, chromosomal localization, phylogenetic

relationship, conserved motif determination, and expression patterns during the leaf expansion period of the camphor tree. Highlighting several novel findings, our work provides a thorough characterization of CcWRKY TFs across the *C. camphora* genome, laying a solid foundation for future research in functional genomics regarding this important tree species.

2. Results

2.1. Identification of WRKY Protein Family

In this study, a total of 72 WRKY candidate proteins were identified in *C. camphora* (Table 1). These candidate proteins were submitted to the NCBI CDD database (Table S1) and the SMART program (Table S2) for conserved domain validations. The results showed that all the 72 candidate proteins contained WRKY domains. These WRKY proteins were renamed, and their physicochemical properties are shown in Table 1. The lengths of CcWRKY proteins varied greatly, ranging from 154 aa (CcWRKY29) to 831 aa (CcWRKY4), with an average length of approximately 379 aa. The molecular weight ranged from 17619.86 Da (CcWRKY29) to 91314.11 Da (CcWRKY4). The isoelectric point (pI) ranged from 4.81 (CcWRKY12) to 9.73 (CcWRKY44), among which 40 pIs < 7 and 32 pIs > 7. The instability index (II) ranged from 30.09 (CcWRKY10) to 70.14 (CcWRKY2). Among them, CcWRKY5/8/10/32/38 had instability indices of less than 40, indicating that they were stable proteins. The aliphatic index ranged from 42.12 (CcWRKY42) to 82.71 (CcWRKY36). The grand average of hydropathicity (GRAVY) ranged from -1.05 (CcWRKY42) to -0.37 (CcWRKY6), indicating that the CcWRKY TFs were all hydrophilic proteins. Subcellular localization predictions indicated that 71 of the 72 CcWRKY proteins were localized in the nucleus, with CcWRKY29 predicted to be in the chloroplast. This suggested that CcWRKY proteins predominantly function in the nucleus (Table 1). Targeting protein predictions showed that only CcWRKY29 contained a signal peptide. Meanwhile, nuclear localization signal (NLS) predictions revealed that 13 of the 72 CcWRKY proteins possessed an NLS motif (Table 1).

In addition, the distribution of 70 CcWRKY genes on 12 chromosomes of *C. camphora* was statistically random overall ($X\text{-squared} = 10.452$, $df = 12$, $p = 0.4602$), while two CcWRKYs (CcWRKY71, CcWRKY72) were not anchored to chromosomes (Figure 1). Nevertheless, we observed a clustered pattern in their distribution. For instance, chromosome 3 contained the largest number of CcWRKYs, with 15 genes showing some clusterings, while chromosome 4 contained nine CcWRKYs, and chromosome 11 had eight CcWRKYs. In contrast, chromosome 9 only contained one CcWRKY gene, and chromosome 12 contained three CcWRKYs (Figure 1).

Table 1. Basic information of CcWRKY TF members.

Gene Name	Gene ID	Amino acids	Molecular weight (Da)	Isoelectric point (pI)	Instability index (II)	Aliphatic index	Grand average of hydropathicity	NLS
CcWRKY1	Ccam01g01320	202	22929.21	6.29	53.73	48.66	-0.92	no
CcWRKY2	Ccam01g01332	279	31328.84	8.23	70.14	47.96	-1.02	no
CcWRKY3	Ccam01g01375	202	23216.22	9.10	40.71	60.79	-0.79	yes
CcWRKY4	Ccam01g03358	831	91314.11	6.09	53.96	68.98	-0.60	no
CcWRKY5	Ccam01g03535	183	20884.51	9.58	34.00	53.22	-0.92	yes
CcWRKY6	Ccam02g00068	305	32859.34	9.67	49.90	66.95	-0.37	no
CcWRKY7	Ccam02g00318	577	63115.17	5.88	51.78	68.28	-0.62	no
CcWRKY8	Ccam02g00335	309	33954.07	6.46	34.75	68.19	-0.69	no
CcWRKY9	Ccam02g00336	278	30788.64	8.13	41.63	72.63	-0.59	no
CcWRKY10	Ccam02g02058	204	22130.84	5.35	30.09	72.21	-0.41	no
CcWRKY11	Ccam02g03195	352	38764.21	9.70	56.43	62.59	-0.71	no
CcWRKY12	Ccam03g00297	447	49627.64	4.81	48.17	60.49	-0.82	no
CcWRKY13	Ccam03g00517	580	62741.96	6.10	56.92	57.03	-0.74	no

CcWRKY14	Ccam03g00678	587	63893.12	7.65	57.10	48.57	-0.81	no
CcWRKY15	Ccam03g00785	318	35629.67	5.88	62.85	56.16	-0.77	yes
CcWRKY16	Ccam03g00786	369	40928.02	6.64	48.93	63.20	-0.58	no
CcWRKY17	Ccam03g01932	185	21015.35	9.51	56.98	50.54	-0.96	yes
CcWRKY18	Ccam03g02460	195	21949.96	8.51	44.02	67.03	-0.63	no
CcWRKY19	Ccam03g02482	344	37433.49	6.33	62.54	56.69	-0.67	no
CcWRKY20	Ccam03g02618	318	35462.09	5.52	64.62	52.20	-0.84	no
CcWRKY21	Ccam03g02853	314	34696.04	6.70	51.94	68.06	-0.56	yes
CcWRKY22	Ccam03g02855	397	43406.46	5.59	54.76	63.58	-0.61	no
CcWRKY23	Ccam03g03394	353	39198.64	9.62	64.56	70.48	-0.66	no
CcWRKY24	Ccam03g03468	206	23872.61	8.16	56.49	45.73	-0.97	no
CcWRKY25	Ccam03g03793	488	54296.39	6.91	54.34	48.38	-0.92	no
CcWRKY26	Ccam03g03866	539	58720.89	7.66	53.06	56.81	-0.81	no
CcWRKY27	Ccam04g00306	471	52258.51	8.87	47.95	62.48	-0.82	no
CcWRKY28	Ccam04g00410	430	47039.08	5.09	42.63	56.05	-0.76	no
CcWRKY29	Ccam04g00759	154	17619.86	8.88	42.03	62.66	-0.70	no
CcWRKY30	Ccam04g01225	310	34539.94	6.60	57.52	73.90	-0.61	no
CcWRKY31	Ccam04g01229	491	53286.15	8.47	57.39	59.86	-0.81	no
CcWRKY32	Ccam04g01721	261	28875.12	7.74	30.20	65.40	-0.79	no
CcWRKY33	Ccam04g01778	302	33464.86	8.97	53.71	65.23	-0.69	no
CcWRKY34	Ccam04g01779	208	23301.12	5.61	56.75	66.59	-0.81	yes
CcWRKY35	Ccam04g02102	654	71102.38	5.68	52.74	64.36	-0.74	no
CcWRKY36	Ccam05g00359	490	55070.47	4.94	54.73	82.71	-0.75	no
CcWRKY37	Ccam05g00959	740	80083.45	6.09	50.14	56.27	-0.73	no
CcWRKY38	Ccam05g02331	165	18405.91	9.72	33.52	63.82	-0.81	no
CcWRKY39	Ccam05g02771	415	45104.08	5.48	42.52	59.71	-0.70	no
CcWRKY40	Ccam05g03164	299	32838.52	5.77	54.63	67.16	-0.66	no
CcWRKY41	Ccam06g01064	182	20838.10	9.37	40.19	51.32	-1.04	yes
CcWRKY42	Ccam06g01432	208	24184.94	8.41	61.09	42.12	-1.05	no
CcWRKY43	Ccam06g01636	334	37415.68	9.52	50.64	65.39	-0.53	no
CcWRKY44	Ccam06g02136	352	39633.05	9.73	62.27	61.19	-0.74	no
CcWRKY45	Ccam07g00975	430	47493.15	5.19	57.10	57.60	-0.76	no
CcWRKY46	Ccam07g01469	596	64053.71	5.73	52.90	59.51	-0.70	no
CcWRKY47	Ccam07g01532	317	35077.74	7.11	57.41	42.78	-0.91	yes
CcWRKY48	Ccam07g01664	267	29370.72	5.76	68.89	52.28	-0.75	no
CcWRKY49	Ccam07g01903	325	36564.64	9.71	55.60	65.11	-0.72	no
CcWRKY50	Ccam08g01789	252	28300.28	9.16	47.47	68.85	-0.62	no
CcWRKY51	Ccam08g01792	317	35249.97	8.74	57.54	63.38	-0.80	no
CcWRKY52	Ccam08g01826	555	59846.56	6.33	55.48	64.20	-0.74	no
CcWRKY53	Ccam08g02171	308	33376.94	9.56	43.95	67.86	-0.51	yes
CcWRKY54	Ccam09g01851	474	52618.54	5.55	46.69	64.85	-0.76	no
CcWRKY55	Ccam10g00062	193	21995.86	9.49	49.33	58.65	-0.81	no
CcWRKY56	Ccam10g00088	336	37554.78	5.84	63.41	54.88	-0.74	no
CcWRKY57	Ccam10g01821	240	27430.30	5.53	58.25	53.12	-1.03	no
CcWRKY58	Ccam10g01879	313	34489.17	5.95	66.23	45.18	-0.87	yes
CcWRKY59	Ccam10g02021	512	55821.95	8.30	51.92	62.97	-0.64	no
CcWRKY60	Ccam11g00131	303	33627.60	5.64	60.15	64.39	-0.68	yes
CcWRKY61	Ccam11g00149	236	26917.31	6.40	54.36	61.48	-0.84	no
CcWRKY62	Ccam11g01089	797	87554.96	6.35	54.73	62.15	-0.72	no
CcWRKY63	Ccam11g01090	706	76678.53	5.86	56.37	61.60	-0.71	no
CcWRKY64	Ccam11g01170	503	54849.97	8.34	56.59	63.92	-0.60	no
CcWRKY65	Ccam11g01283	242	27323.35	5.88	61.00	51.07	-0.88	yes
CcWRKY66	Ccam11g01643	472	52370.07	8.97	48.45	62.75	-0.92	no
CcWRKY67	Ccam11g01901	742	79958.11	5.70	50.01	56.99	-0.71	no

CcWRKY68	Ccam12g00109	557	61024.06	6.23	53.05	61.38	-0.69	no
CcWRKY69	Ccam12g00173	336	36891.77	8.67	60.18	45.86	-0.91	yes
CcWRKY70	Ccam12g00336	276	30345.67	5.12	63.80	52.03	-0.75	no
CcWRKY71	Ccam00g00092	572	62699.88	6.85	49.20	58.72	-0.72	no
CcWRKY72	Ccam00g00207	287	31649.25	4.83	47.47	57.07	-0.53	no

Footnote: All the CcWRKY TFs were located at the nucleus and contained no targeting proteins except for CcWRKY29 (chloroplast, signal peptide).

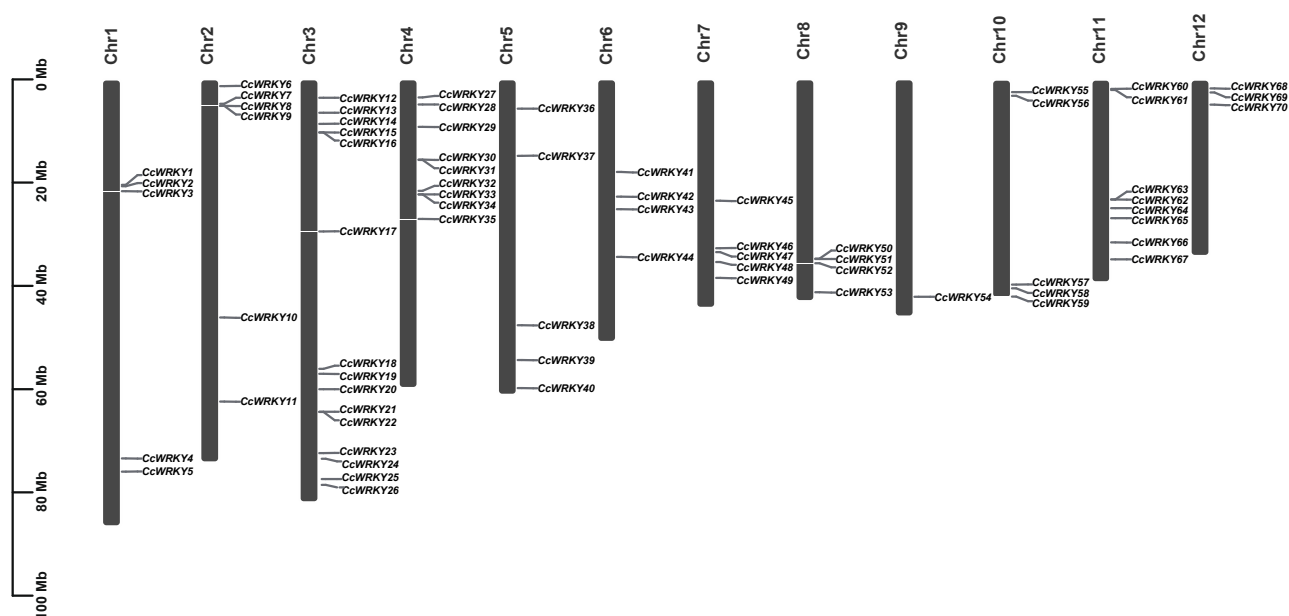


Figure 1. The distribution of CcWRKY genes on chromosomes. The scale bar on the left corresponds to the length of the chromosomes.

2.2. Classification and Phylogenetic Analysis

The phylogenetic analysis showed that CcWRKY proteins were divided into three groups (I, II, and III), and group II contained five subgroups (IIa, II b, II c, II d, and IIe) (Figure 2). Among these groups, group III was clustered with group IId + IIe. Members of different subfamily CcWRKY TFs clustered with the corresponding AtWRKY subfamilies. There were 14 AtWRKY proteins and 14 CcWRKY proteins in group I. Also, the number of CcWRKY proteins was the same as that of AtWRKY proteins in group IIb (both of them were eight). There were 17 AtWRKY proteins and 15 CcWRKY proteins in group IIc, seven AtWRKY proteins and nine CcWRKY proteins in group IId, eight AtWRKY proteins and nine CcWRKY proteins in group IIe, and 14 AtWRKY proteins and 11 CcWRKY proteins in group III. However, in group IIa, there were three AtWRKY proteins, whereas the number of CcWRKY proteins was six, which was twice the number of AtWRKY. Though the number of WRKY TFs varied between *C. camphora* and *A. thaliana* across different groups, the chi-square test demonstrated that the difference was not statistically significant ($X^2_{squared} = 1.7869$, $df = 6$, $p = 0.9382$).

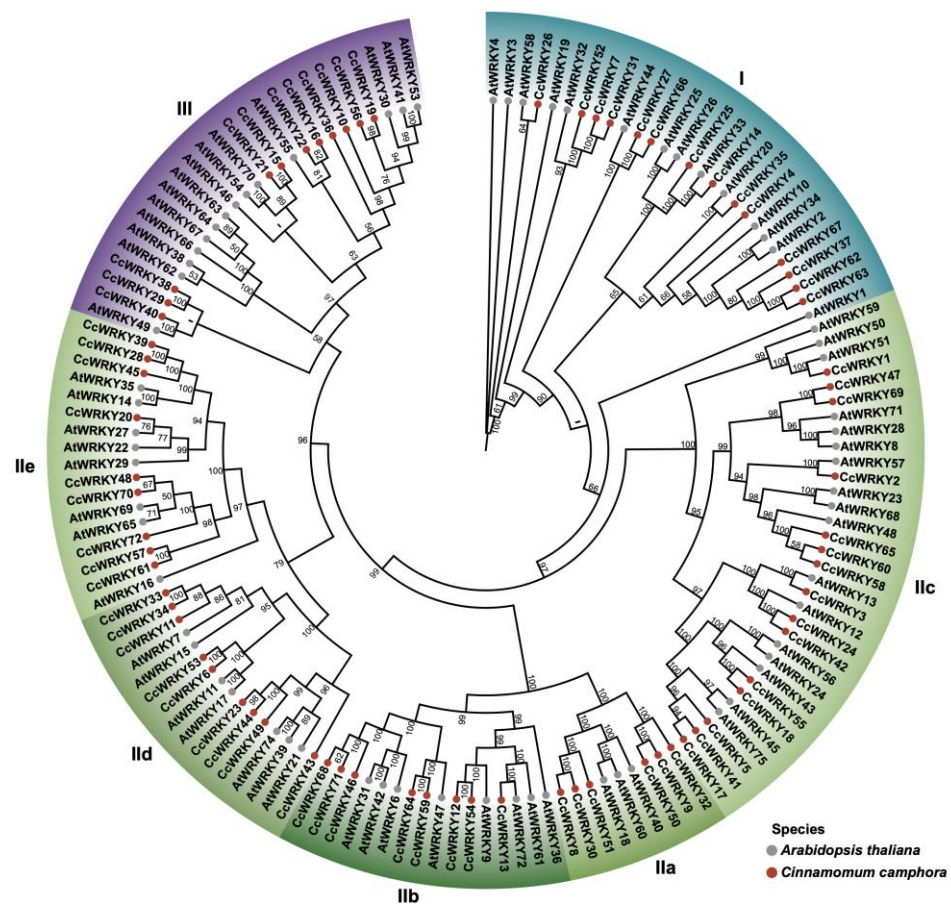


Figure 2. Phylogenetic tree of WRKY family in *C. camphora* and *A. thaliana*. The consensus maximum likelihood (ML) phylogenetic tree was inferred using IQ-TREE with 1000 ultra-fast bootstrap (BS) replicates. The WRKY proteins were clustered into three groups (I, II, and III), and group II contained five subgroups (II a, II b, II c, II d, and II e). The different species and groups are indicated by different colors. The BS values of nodes are shown.

2.3. Motif Analysis of the WRKY in *C. camphora*

The visualization and comparison of 72 CcWRKY protein sequences showed that most of the TFs contained a highly conserved heptapeptide, WRKYGQK, and a zinc finger motif (C₂H₂ type/C₂HXC type) (Figure S1), while some sequence variations occurred (Figure S2). Specifically, the corresponding heptapeptides for CcWRKY1/10/29/34/38 were WRKYGKK, WRKYAQE, WKKYGQK, GKKYGQK, and WKKYGQK, respectively. Furthermore, we did not observe a corresponding zinc finger structure following the conserved heptapeptide sequences in CcWRKY6 and WRKY10.

Subsequently, we identified ten conserved motifs among 72 CcWRKY TFs (Figures 3 and S3). Motif 1 and motif 3 represented the conserved heptapeptide WRKYGQK, while motif 2 contained most of the zinc finger structure. Collectively, motif 1 and motif 2 formed a conserved WRKY domain (Figure S3). Generally, most CcWRKY proteins (70 out of 72) possessed both motif 1 and motif 2. Additionally, group III not only had motif 1 and motif 2 but also possessed motif 3, corresponding to two WRKY domains. Furthermore, we found that the motif composition and distribution were relatively conservative among members within the same clade. For example, motifs 1/2/5/7 were present in every WRKY protein in the IIa subgroup clade, with motif 1 and motif 2 located between motif 5 and motif 7, motif 5 located at the N-terminal, and motif 7 located at the C-terminal of the WRKY protein sequences. This indicates that motif patterns could be related to the function of WRKY proteins. Meanwhile, closely related clades shared motif similarities

Figure 3. Conserved motifs for CcWRKY proteins in *C. camphora*. Different motifs are shown with colored boxes and numbers (1–10). The lines represent the non-conserved sequences. The lengths of motifs can be estimated using the scale at the bottom.

2.4. Identification of Differential Expression Patterns of WRKY Genes

We isolated total RNA from tree leaves collected from healthy camphor trees during three distinct leaf-expansion stages (Figure 4A). Qualified RNA samples were subject to RNA sequencing, and an average of 6.06 Gb of clean data (see Materials and Methods) were generated for each sample (Table S4).

Using these transcriptomic data, we conducted differential gene expression (DGE) analyses between S1 and S2 and between S1 and S3 (Figure 4B). In total, 1062 up-regulated genes were found between S1 and S2, which were enriched in 51 gene ontology (GO) terms relating to ‘Biological processes’; meanwhile, 1279 up-regulated genes were found between S1 and S3, which were enriched to 66 GO terms (Table S5) relating to ‘Biological processes’. Notably, 34 enriched GO terms were present between both S1-S2 and S1-S3, some of which were related to the response to temperature, abscisic acid, light stimulus, and cell wall development (Table S5). Specifically, we found three (*CcWRKY24*, *CcWRKY42*, *CcWRKY70*) and five (*CcWRKY24*, *CcWRKY42*, *CcWRKY48*, *CcWRKY58*, *CcWRKY70*) CcWRKYs genes that were up-regulated from the S1 to the S2 stage and from the S1 to the S3 stage, respectively (Table S6 and S7). We focused the subsequent validation analysis on *CcWRKY24*, *CcWRKY42*, and *CcWRKY70* genes, considering that these three genes exhibited up-regulation from S1 to S2 as well as from S1 to S3 ($\log_2[\text{Fold Change (FC)}] > 1$; $p_{\text{adj}} < 0.05$) (Figure 4B).

The heatmap results based on the transcripts per kilobase per million mapped reads (TPM) profile showed that these three genes exhibited relatively low expression levels in the S1 stage. The expression level of *CcWRKY42* was higher in the S2 and S3 stages compared with the S1 stage, while the expression level of *CcWRKY24* gradually increased from the S1 to the S3 stage. The expression level of *CcWRKY70* increased from the S1 stage to the S2 stage and was similar between the S2 and the S3 stage (Figure 4C, Table S8).

Furthermore, the qPCR experiments showed that the expression profiles of these three genes were consistent with those predicted by transcriptome data. The one-way ANOVA indicated that the expression levels of *CcWRKY24* ($F = 1790$, $df = 8$, $p < 0.001$), *CcWRKY42* ($F = 46.35$, $df = 8$, $p = 0.001$), and *CcWRKY70* ($F = 11.07$, $df = 8$, $p < 0.01$) among the three time periods were significantly different (Table S9). Multiple comparisons (Tukey’s post-hoc analysis) indicated that the relative expression level of *CcWRKY24* and *CcWRKY42* increased sequentially from S1 to S3 ($p < 0.05$), while that of *CcWRKY70* was higher in S2 and S3 compared to S1 ($p < 0.05$) and no significant difference was found between the latter two stages (Figure 4D).

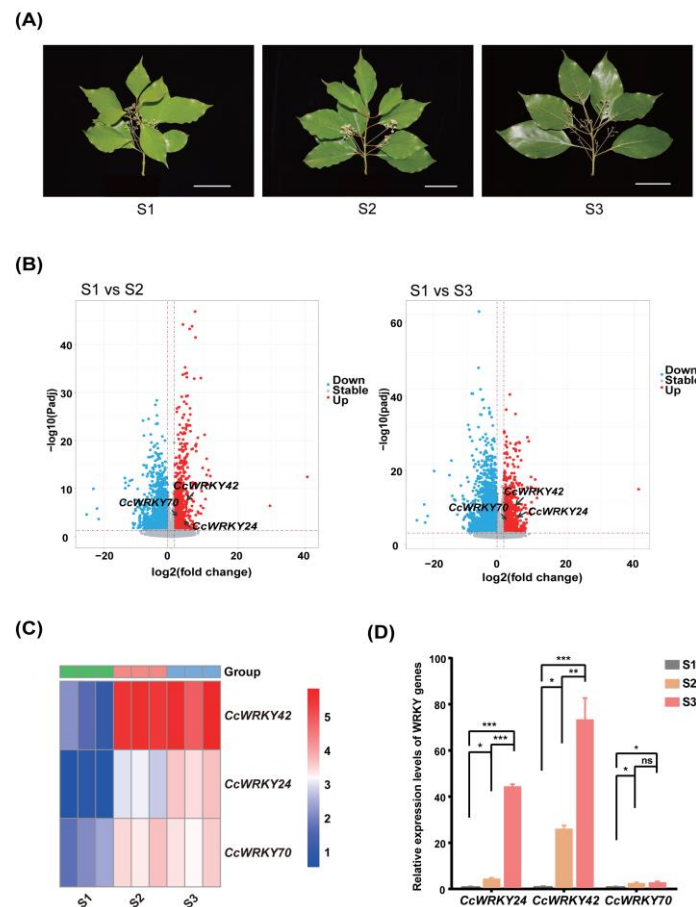


Figure 4. (A) The morphological illustrations of *C. camphora* at three stages of leaf development. Scale bar: 5 cm. (B) Volcano plots displaying the DEGs between different stages. Each point on the plot represents an individual gene, with the x-axis indicating the $\log_2\text{FC}$ in gene expression and the y-axis showing the statistical significance ($-\log_{10}p_{\text{adj}}$). (C) The predicted expression of *CcWRKY24*, *CcWRKY42*, and *CcWRKY70* at three stages. TPM values for *CcWRKY* genes were log-transformed. The heatmap corresponds to gene expression levels. (D) Relative expression levels of three *CcWRKY* genes quantified by qPCR. Error bars indicate standard errors of three biological replicates. Asterisks indicate the significance of the expression level difference among stages ($^{\text{ns}} p > 0.05$, $^* p < 0.05$, $^{**} p < 0.01$, $^{***} p < 0.001$).

3. Discussion

The WRKY TF family, one of the essential classes of TFs in plants, plays an indispensable role in plant growth, development, and stress response [4,44]. With the continuous expansion of relevant research, the genome-wide analysis of the WRKY gene family has been conducted in numerous species, among which the number of identified WRKY proteins differed. For example, there are more than 70 WRKY proteins in *Arabidopsis* [45], 58 in eggplant [46], 79 in potato [47], 109 in rice [48], and 185 in soybean [49]. In this study, 72 WRKY proteins were identified in *C. camphora*, which was comparable to those identified in *Arabidopsis* and potato but less than that in rice and soybean.

The prediction of physicochemical properties for 72 *CcWRKY* TFs indicated that 40 proteins were acidic ($\text{pI} < 7$), 32 were alkaline ($\text{pI} > 7$), and most (67 out of 72) were unstable (Table 1). Furthermore, there were also differences in the length, molecular weight, and aliphatic index of the 72 *CcWRKY* TFs identified (Table 1). Despite the variation in the physicochemical properties of these proteins, they were determined to be hydrophilic, which is similar to what was found by Guo et al. [50]. The observed variation in the physicochemical properties of these *CcWRKY*s indicates the structural complexity and functional divergence among them, which is consistent with the literature [51]. The structural

complexity and functional diversity among CcWRKYs imply their versatile physiological roles and regulatory functions within the plant. Therefore, a deeper understanding of the structures and functions of CcWRKYs can help us gain better insights into the growth, development, and environmental stress response mechanisms of the camphor tree, as suggested by the study on tobacco. Additionally, the analysis of conserved domains revealed that almost all the CcWRKY genes possessed motif 1 and motif 2, which together formed a single WRKY conserved domain (Figures 3, S1, and S3). This reflects the structural conservatism of CcWRKY TFs. Meanwhile, the same clade or closely related clades shared motif similarities, while possessing subgroup-specific motifs (Figure 3). This finding is similar to those reported by Guo et al. [50] and Hu et al. [52], which could partly explain the pattern of functional diversification in WRKY TFs. The majority of CcWRKY TFs were located at the nucleus, as subcellular localization predictions showed (Table 1), suggesting that CcWRKY TFs likely play a primary role in transcriptional regulation within the nucleus. Yang et al. [41] identified 3 TPS (*CcTPS1*, *CcTPS3*, *CcTPS4*) and 37 other genes (including 5 WRKY, 15 MYB, 10 ERF/AP2, 5 bZIP, and 2 BHLH) that may be crucially involved in the biosynthesis and regulation of monoterpenes in *C. camphora*. Chen et al. [53] discovered that AtGPPS11 and AtGPPS12 interacted to regulate monoterpene biosynthesis in *Arabidopsis* flowers. Meanwhile, AtWRKY12 and AtWRKY13 interacted with SPL10 to modulate the age-mediated flowering process [27]. These findings imply putative interactions between CcWRKY and other TFs as well as within the CcWRKYs.

In our study, the phylogenetic analysis revealed that the members of CcWRKYs clustered with their corresponding *Arabidopsis* subfamilies (Figure 2). Specifically, CcWRKYs were categorized into three groups (groups I, II, and III). Group II can be further divided into five subgroups (IIa, IIb, IIc, IId, IIe). Among these five subgroups, group IIa was sister to group IIb, group IId was sister to group IIe, group IIc exhibited an orphan clade, while group III was nested within group II. This is consistent with the classification of *A. thaliana* [4–6], indicating that the identification and classification of the 72 CcWRKYs are reliable and that the WRKY TF families in *C. camphora* and *A. thaliana* share similar evolutionary processes and a high degree of conservatism.

The literature shows that group IIc harbors a greater sequence diversity than other subgroups in group II [3]. Similarly, their functions are also diverse. In our study, the phylogenetic analysis showed that both CcWRKY24 and CcWRKY42 belong to group IIc, which are orthologs of AtWRKY12 (Figure 2). Functionally, AtWRKY12 and AtWRKY13, a paralogous pair of TFs, likely play a role in the transition from a vegetative phase to a reproduction phase [2,27]. For example, the knockout of the *AtWRKY12* gene could delay the flowering time, while the loss of the *AtWRKY13* function would accelerate the flowering process [27,28]. Meanwhile, they also play different roles in stem development [2]. In our study, as the leaves developed from S1 to S3, the floral organs continued to develop at the same time (Figure 4A). Therefore, CcWRKY24 and CcWRKY42 were presumed to be involved in the regulation of plant growth associated with the development of both vegetative and reproductive organs. Additionally, phylogenetic analysis showed that CcWRKY70 was close to AtWRKY14, AtWRKY35, AtWRKY65, and AtWRKY69, all of which belong to subgroup IIe (Figure 2). Previous research indicates that WRKY14 (ABT1) is an important regulator of thermomorphogenesis in *Arabidopsis*, and its close homologs WRKY35 (ABT2), WRKY65 (ABT3), and WRKY69 (ABT4) also play critical roles in this responding process [54]. Therefore, we speculate that CcWRKY70 could also play a key role in plant thermomorphogenesis (which is also tightly linked to leaf expansion), enabling *C. camphora* to achieve coordinated growth under various combinations of temperature, light, and other environmental conditions. However, whether CcWRKY24/42/70 possesses these functions remains to be functionally validated. Functional analysis methods such as gene knockout and overexpression can be considered in future work.

The roots, bark, and leaves of *C. camphora* are rich in essential oils, which mainly comprise monoterpenes and sesquiterpenes [55]. During the processes of leaf growth and floral organ development in the camphor tree, there would be an accumulation of

terpenoids and aromatic compounds. It is widely acknowledged that terpenoids and aromatic compounds, as important constituents of plant secondary metabolites, have significant implications for the economic value and ecological functions of plants, including the camphor tree [56], the Arabian jasmine (*Jasminum sambac*) [57], the Chinese mahogany (*Toona sinensis*) [58], and the sweet osmanthus (*Osmanthus fragrans*) [59]. These compounds not only endow plants with unique aromas and flavors but also play a crucial role in plant stress resistance, defense mechanisms, and interactions with other organisms [60–62]. It is acknowledged that the WRKY TFs play pivotal roles in regulating these secondary metabolites. For instance, studies have indicated that WRKY genes may be involved in aroma synthesis by regulating the production of terpenes and aromatic volatiles [63–65]. Lu et al. [64] suggested that overexpression of *JsWRKY51* is a crucial factor in enhancing the accumulation of β -ocimene, an important aromatic terpene component in *Jasminum sambac*. Regarding the synthesis and accumulation of these compounds, several studies have revealed that a large number of volatile compounds are gradually synthesized and accumulated during the bud-to-full-blooming flowering stages [57,66,67]. Specifically, Lu et al. [64] discovered that some WRKY genes were highly expressed in full-blooming flowers, as well as being significantly associated with the accumulation of multiple terpenoid compounds at the blooming stage. Meanwhile, Ding et al. [63] showed that eight *OfWRKYs* participated in regulating flowering in the sweet osmanthus. Among these eight genes, the expression patterns of *OfWRKY7/19/36/139* were correlated with specific monoterpenes. Therefore, we speculate that CcWRKY TFs may be involved in the development of both leaf and floral organs in the camphor tree, as well as the accumulation of secondary metabolites. Although this study did not include metabolomic data, we strongly recommend that future studies integrate metabolomic data to further investigate the functional dynamics of WRKY genes during the leaf expansion stage or other development periods. This approach will help provide a more comprehensive understanding of the role of WRKY genes in plant growth and offer deeper insights into their complex regulatory networks.

Moreover, we found that three genes (*CcWRKY24*, *CcWRKY42*, *CcWRKY70*) continuously exhibited up-regulation across three leaf expansion stages. Given that WRKY genes may also play roles in other regulation pathways related to photosynthesis, which could retain stable expressions during leaf expansion, the number of identified CcWRKY genes with differential expressions among conditions is reasonable and aligns with the biological context. Furthermore, the qPCR experiments confirmed that the expression level of *CcWRKY24* increased gradually from S1 to S3, while *CcWRKY42* and *CcWRKY70* demonstrated higher expression levels in S2 and S3 than in S1. This suggests that these three genes may be involved in various regulation pathways during the expansion of leaves. Additionally, studies have shown that WRKY TFs mediate morphogenesis during the vegetative growth phase of plants. For example, *AtWRKY44* is a crucial regulator of early trichome development [68] and *AtWRKY71* plays an important role in shoot branching [69]. Research on the role of WRKY TFs in leaf expansion is extremely scarce, but our current study has provided a foundation for future work to build on. In summary, our study appears to be the first one to investigate WRKY TFs across the *C. camphora* genome, profiling their gene expression during the leaf expansion phase and setting the stage for functional analyses of these and other TFs in the camphor tree.

4. Materials and Methods

4.1. Identification and Physicochemical Properties Analysis

Available AtWRKY protein sequences were obtained from the Arabidopsis Information Resource database (TAIR, <http://www.arabidopsis.org/>, accessed on 27 February 2024). Then, we downloaded the Hidden Markov Model for WRKY TFs (PF03106) from the Pfam website (v. 36.0) (<http://pfam.xfam.org/>, accessed on 27 February 2024) [70]. Subsequently, we used the Blast program (a cutoff of $E \leq 1 \times 10^{-5}$) and the Simple HMM search

program available from Tbttools software (v. 2.064) [71] to identify WRKY family members from the whole genome of *C. camphora* [34] (<https://doi.org/10.6084/m9.figshare.20647452.v1>, accessed on 27 February 2024). The search results were merged, and the intersection was taken as candidate proteins. These candidate proteins were submitted to the NCBI CDD database [72] and the Batch SMART program in Tbttools for validation of conserved domains. The physicochemical properties and the subcellular localization information of the WRKY TFs were analyzed by the Online Tool ExPASy [73] and the WOLF PSORT tool [74], respectively. TargetP-2.0 was used to predict the presence of targeting proteins [75]. The NLS motifs were predicted using the NLStradamus tool [76]. We used the Gene Location Visualize module from the GFF program in Tbttools to visualize the distribution of *CcWRKY* genes on chromosomes. Additionally, we performed a chi-square test to determine whether these WRKY genes were randomly distributed across these chromosomes with the `chisq.test` function from the R package `stats` (v. 4.1.2) [77].

4.2. Phylogenetic Tree Analysis

The WRKY protein sequences of *C. camphora* and *A. thaliana* were aligned using MAFFT (v. 7.508; --auto) [78] and then trimmed using trimAl (v. 1.4; -automated1) [79]. Next, the consensus maximum likelihood (ML) phylogenetic tree was inferred using IQ-TREE (v. 2.2.0.3) with 1000 ultra-fast bootstrap (BS) replicates [80,81]. The best-fit protein substitution model was determined automatically with ModelFinder as supported by IQ-TREE (JTT+F+I+R6) (-m MFP) [82]. The phylogenetic tree was visualized using the tvBOT Online Tool [83]. Furthermore, we performed a chi-square test to examine whether the numbers of WRKY TFs differed between the camphor tree and *A. thaliana* among groups with the `chisq.test` function from the R package `stats`.

4.3. Analysis of Conserved Motifs of *CcWRKY* TFs

The WebLogo tool (v. 2.8.2) [84] was used to visualize the sequences of the conserved *CcWRKY* domains. Later, these sequences were compared by the Jalview program (v. 2.11.4.1) [85] after being aligned with the Clustal Omega program (v. 1.2.4) available from the EMBL-EBI Job Dispatcher [86]. The neighbor-joining (NJ) tree of *CcWRKY* proteins was inferred using MEGA11 [87]. The conserved motifs of WRKY TFs were predicted by the MEME analysis suite (v. 5.5.5) [88] with the number of motifs set to 10. Subsequently, the results were visualized by tvBOT. In addition, the *cis*-acting regulatory elements (2000 bp upstream from the starting codon) of the *CcWRKY* genes were searched by the PlantCARE tool [89].

4.4. Sample Collection and Transcriptome Sequencing

To analyze the *CcWRKY* gene expression profiles during leaf expansion, we collected healthy leaves of *C. camphora* at three different stages (S1: 10 AM, 9 April 2024; S2: 10 AM, April 24, 2024; S3: 10 AM, 7 May 2024) at Taizhou University, Zhejiang Province. All these days were sunny days. Compared to the preceding week (2 April 2024; 17 °C), temperatures at the three sampling points progressively increased (S1: 19 °C; S2: 21 °C; S3: 23 °C). Three biological replicates for every stage were sampled. The three sampled trees were all planted in 2004, sourced from the same nursery, and propagated from the same cloned genotype. Currently, the trees are approximately eight meters tall. They were planted in an open, sun-exposed area on the campus, growing side by side with no shading between them. Branches with flowers from the uniformly sunlit side of the trees were collected, and adjacent leaves near the floral organs were harvested. The leaves were immediately stored in liquid nitrogen upon collection and were kept frozen until RNA extraction. These leaf samples were sent to a commercial sequencing institute (Annoroad Gene Technology Co., Ltd., Beijing, China) for RNA extraction and transcriptome sequencing. The total RNA was extracted based on the pBIOZOL methods

(<https://www.protocols.io/view/rna-isolation-from-plant-tissue-protocol-7-pbiozol-81wgb1e9yvpk/v1>). The purity, concentration, and integrity of RNA products were determined with a Nanodrop2000 microspectrophotometer and a Labchip GX touch microfluidic capillary system. Following the manufacturer's protocol and the literature, RNA samples with OD260/OD280 ratio of ca. 2.0, total RNA amount > 1 µg, and RNA integrity number (RIN) > 6 were considered qualified [90]. Different RNA libraries were pooled according to the effective concentration and the target downstream data volume and then sequenced on the DNBSEQ™-T7 instrument to generate 150 bp paired-end reads. Adapter reads, reads containing ambiguous bases, and low-quality reads (bases with $Q \leq 20$ accounted for more than 50% of the entire read length) were removed from the raw sequencing data with in-house scripts available in the sequencing institute.

4.5. Differential Expression Patterns of *CcWRKY* Genes

To investigate DEGs between these leaf expansion stages (S1-S3), we mapped clean transcriptomic reads to the *C. camphora* genome using HISAT2 (v. 2.2.1) [91]. Subsequently, we analyzed the expression levels of genes using StringTie (v. 2.2.1) [92]. The read count information was extracted using the prepDE.py script available in StringTie (Table S10). Based on the count information file, the DEGs were identified using the R package DESeq2 (v. 1.34.0) [93] based on the criteria of $|\log_2FC| > 1$ and $p_{adj} < 0.05$. Next, we annotated these DEGs by querying against *A. thaliana* and then enriched them to test whether these genes were statistically strongly associated with the GO terms. Annotation and enrichment analysis were conducted using KOBAS-i [94]. The GO terms under the 'biological process' category were focused on, and only those with Fisher's exact test (with Benjamini and Hochberg FDR correction) p -value < 0.05 were kept. Meanwhile, we plotted a volcano plot and identified the upregulated *WRKY* genes between stages based on the results of our DEG analysis. To investigate the differences in expression levels of these upregulated genes during these stages, we utilized the getTPM.py script available in StringTie to perform normalization of read counts and gene lengths, thereby eliminating the impacts of sequencing depth and gene length biases, resulting in a TPM profile. The heatmap based on the TPM profile and the volcano plots were generated using the RNA-diff module (v1.1.0) (<https://github.com/nongxinshengxin/RNAdiffAPP>, accessed on 20 July 2024) available from TBtools.

4.6. Quantitative Real-time Polymerase Chain Reaction (qPCR)

To verify the expression differences of three *CcWRKY* genes that were up-regulated between both S1-S2 and S1-S3, we conducted a qPCR analysis using the mRNA dye-based method (with the intercalating of SYBR Green) [95]. The RNA was extracted from leaves that were used for the RNA-seq as described above. We used the FastKing RT Kit (with gDNase) (TIANGEN Biotech, Co., Ltd., Beijing, China) to remove gDNA and synthesize cDNA by following the manufacturer's protocol. The *CcActin* gene was used as the reference gene for qPCR [41]. The primers for the selected *CcWRKY* genes were designed using the online software primer3 (v. 0.4.0) (Table S11) [96].

The qPCR was performed on a CFX96™ Real-Time System (Bio-Rad Laboratories, Inc., Hercules, CA, USA) using the ChamQ Universal SYBR qPCR Master Mix (Vazyme Biotech, Co., Ltd., Nanjing, China). The qPCR conditions consisted of initial denaturation at 95°C for 10 s, followed by 40 cycles of denaturation at 95°C for 10 s, and then annealing and extension at 60°C for 30 s. Then, we performed a melting curve analysis to determine the specificity of the reactions. The relative expression of each gene was calculated by the $2^{-\Delta\Delta Ct}$ method [97]. The expression levels of genes in S1 were set as the reference. Finally, we tested whether gene expression levels differed among the three stages with one-way ANOVA and Tukey's post-hoc analysis using R package stats.

5. Conclusions

Through a comprehensive genome-wide study of the WRKY gene family in the camphor tree, we developed a fundamental understanding of their physicochemical properties and structural characteristics, phylogenetic relationships, and gene expression profiles during leaf expansion. The transcriptional up-regulation of certain *CcWRKY* genes during leaf expansion suggests their regulatory role in this important developmental phase. In the future, functional analyses of these WRKY TFs in *C. camphora* should be conducted to better understand their roles in leaf expansion and additional developmental phases. Despite some limitations, this study lays a solid foundation for further investigations into the regulatory mechanisms of WRKY TFs in the camphor tree.

Supplementary Materials: The following supporting information can be downloaded at: www.mdpi.com/xxx/s1, Table S1: Results of conserved domain validation against the NCBI CDD database; Table S2: Results of conserved domain validation from the SMART program; Table S3 Information of *cis*-elements present in *CcWRKY* genes. Table S4: A summary of RNA samples and sequencing data; Table S5: Significantly enriched Gene Ontology terms (biological process) of DEGs between different stages; Table S6: The change of gene expression level between S1 and S2; Table S7: The change of gene expression level between S1 and S3; Table S8: TPM matrix of assembled transcripts among three stages; Table S9: Quantification Cq values from the qPCR experiments; Table S10: Gene count information at different stages; Table S11: Primer information of three targeted genes in the qPCR validation; Figure S1: Conserved domain logo of *CcWRKY* TFs; Figure S2: Comparison of WRKY domain sequences among 72 *CcWRKY* TFs; Figure S3: Ten types of conserved motifs in *CcWRKY* TFs. Figure S4: The *cis*-acting regulatory elements in *CcWRKY* genes.

Author Contributions: Conceptualization, H.L.; methodology, S.L. and J.J.; software, S.L.; validation, S.L. and H.L.; formal analysis, S.L. and J.J.; investigation, S.L. and H.L.; resources, H.L.; data curation, S.L.; writing—original draft preparation, S.L. and J.J.; writing—review and editing, S.L. and H.L.; visualization, S.L.; supervision, H.L.; project administration, H.L.; funding acquisition, H.L. All authors have read and agreed to the published version of the manuscript.

Funding: This research was funded by the National Natural Science Foundation of China, grant number 32100164.

Data Availability Statement: The data presented in this study are openly available in GenBank under the BioProject accession number PRJNA1164943.

Acknowledgments: The authors thank Junmin Li for the assistance in computational resources.

Conflicts of Interest: The authors declare no conflicts of interest.

References

1. Ishiguro, S.; Nakamura, K. Characterization of a cDNA Encoding a Novel DNA-Binding Protein, SPF1, That Recognizes SP8 Sequences in the 5' Upstream Regions of Genes Coding for Sporamin and β -Amylase from Sweet Potato. *Mol. Gen. Genet. MGG* **1994**, *244*, 563–571. <https://doi.org/10.1007/BF00282746>.
2. Wang, H.; Chen, W.; Xu, Z.; Chen, M.; Yu, D. Functions of WRKYs in Plant Growth and Development. *Trends Plant Sci.* **2023**, *28*, 630–645. <https://doi.org/10.1016/j.tplants.2022.12.012>.
3. Song, H.; Cao, Y.; Zhao, L.; Zhang, J.; Li, S. Review: WRKY Transcription Factors: Understanding the Functional Divergence. *Plant Sci.* **2023**, *334*, 111770. <https://doi.org/10.1016/j.plantsci.2023.111770>.
4. Eulgem, T.; Rushton, P.J.; Robatzek, S.; Somssich, I.E. The WRKY Superfamily of Plant Transcription Factors. *Trends Plant Sci.* **2000**, *5*, 199–206. [https://doi.org/10.1016/S1360-1385\(00\)01600-9](https://doi.org/10.1016/S1360-1385(00)01600-9).
5. Rushton, P.J.; Somssich, I.E.; Ringler, P.; Shen, Q.J. WRKY Transcription Factors. *Trends Plant Sci.* **2010**, *15*, 247–258. <https://doi.org/10.1016/j.tplants.2010.02.006>.
6. Zhang, Y.; Wang, L. The WRKY Transcription Factor Superfamily: Its Origin in Eukaryotes and Expansion in Plants. *BMC Evol. Biol.* **2005**, *5*, 1. <https://doi.org/10.1186/1471-2148-5-1>.
7. Rogers, H.J. From Models to Ornamentals: How Is Flower Senescence Regulated? *Plant Mol. Biol.* **2013**, *82*, 563–574. <https://doi.org/10.1007/s11103-012-9968-0>.
8. Chen, F.; Hu, Y.; Vannozzi, A.; Wu, K.; Cai, H.; Qin, Y.; Mullis, A.; Lin, Z.; Zhang, L. The WRKY Transcription Factor Family in Model Plants and Crops. *CRC Crit. Rev. Plant Sci.* **2017**, *36*, 311–335. <https://doi.org/10.1080/07352689.2018.1441103>.

9. Woo, H.R.; Kim, H.J.; Lim, P.O.; Nam, H.G. Leaf Senescence: Systems and Dynamics Aspects. *Annu. Rev. Plant Biol.* **2019**, *70*, 347–376. <https://doi.org/10.1146/annurev-arplant-050718-095859>.
10. Luo, M.; Dennis, E.S.; Berger, F.; Peacock, W.J.; Chaudhury, A. MINISEED3 (MINI3), a WRKY Family Gene, and HAIKU2 (IKU2), a Leucine-Rich Repeat (LRR) KINASE Gene, Are Regulators of Seed Size in Arabidopsis. *Proc. Natl. Acad. Sci. USA* **2005**, *102*, 17531–17536. <https://doi.org/10.1073/pnas.0508418102>.
11. Gu, Y.; Li, W.; Jiang, H.; Wang, Y.; Gao, H.; Liu, M.; Chen, Q.; Lai, Y.; He, C. Differential Expression of a WRKY Gene between Wild and Cultivated Soybeans Correlates to Seed Size. *J. Exp. Bot.* **2017**, *68*, 2717–2729. <https://doi.org/10.1093/jxb/erx147>.
12. Lei, R.; Li, X.; Ma, Z.; Lv, Y.; Hu, Y.; Yu, D. Arabidopsis WRKY2 and WRKY34 Transcription Factors Interact with VQ20 Protein to Modulate Pollen Development and Function. *Plant J.* **2017**, *91*, 962–976. <https://doi.org/10.1111/tpj.13619>.
13. Yang, Y.; Chi, Y.; Wang, Z.; Zhou, Y.; Fan, B.; Chen, Z. Functional Analysis of Structurally Related Soybean GmWRKY58 and GmWRKY76 in Plant Growth and Development. *J. Exp. Bot.* **2016**, *67*, 4727–4742. <https://doi.org/10.1093/jxb/erw252>.
14. Cheng, Y.; JalalAhamed, G.; Yu, J.; Yao, Z.; Ruan, M.; Ye, Q.; Li, Z.; Wang, R.; Feng, K.; Zhou, G.; et al. Putative WRKYs Associated with Regulation of Fruit Ripening Revealed by Detailed Expression Analysis of the WRKY Gene Family in Pepper. *Sci. Rep.* **2016**, *6*, 39000. <https://doi.org/10.1038/srep39000>.
15. Tiika, R.J.; Wei, J.; Ma, R.; Yang, H.; Cui, G.; Duan, H.; Ma, Y. Identification and Expression Analysis of the WRKY Gene Family during Different Developmental Stages in *Lycium ruthenicum* Murr. *Fruit. PeerJ* **2020**, *8*, e10207. <https://doi.org/10.7717/peerj.10207>.
16. Ay, N.; Irmeler, K.; Fischer, A.; Uhlemann, R.; Reuter, G.; Humbeck, K. Epigenetic Programming via Histone Methylation at WRKY53 Controls Leaf Senescence in Arabidopsis Thaliana. *Plant J.* **2009**, *58*, 333–346. <https://doi.org/10.1111/j.0960-7412.2009.03782.x>.
17. Brusslan, J.A.; Rus Alvarez-Canterbury, A.M.; Nair, N.U.; Rice, J.C.; Hitchler, M.J.; Pellegrini, M. Genome-Wide Evaluation of Histone Methylation Changes Associated with Leaf Senescence in Arabidopsis. *PLoS ONE* **2012**, *7*, e33151. <https://doi.org/10.1371/journal.pone.0033151>.
18. Fan, Z.; Tan, X.-L.; Shan, W.; Kuang, J.; Lu, W.; Chen, J. Characterization of a Transcriptional Regulator, BrWRKY6, Associated with Gibberellin-Suppressed Leaf Senescence of Chinese Flowering Cabbage. *J. Agric. Food Chem.* **2018**, *66*, 1791–1799. <https://doi.org/10.1021/acs.jafc.7b06085>.
19. Price, A.M.; Aros Orellana, D.F.; Salleh, F.M.; Stevens, R.; Acock, R.; Buchanan-Wollaston, V.; Stead, A.D.; Rogers, H.J. A Comparison of Leaf and Petal Senescence in Wallflower Reveals Common and Distinct Patterns of Gene Expression and Physiology. *Plant Physiol.* **2008**, *147*, 1898–1912. <https://doi.org/10.1104/pp.108.120402>.
20. Meng, L.; Yang, H.; Yang, J.; Wang, Y.; Ye, T.; Xiang, L.; Chan, Z.; Wang, Y. Tulip Transcription Factor TgWRKY75 Activates Salicylic Acid and Abscisic Acid Biosynthesis to Synergistically Promote Petal Senescence. *J. Exp. Bot.* **2024**, *75*, 2435–2450. <https://doi.org/10.1093/jxb/erae021>.
21. Wu, X.; Shiroto, Y.; Kishitani, S.; Ito, Y.; Toriyama, K. Enhanced Heat and Drought Tolerance in Transgenic Rice Seedlings Overexpressing OsWRKY11 under the Control of HSP101 Promoter. *Plant Cell Rep.* **2009**, *28*, 21–30. <https://doi.org/10.1007/s00299-008-0614-x>.
22. Ma, P.; Guo, G.; Xu, X.; Luo, T.; Sun, Y.; Tang, X.; Heng, W.; Jia, B.; Liu, L. Transcriptome Analysis Reveals Key Genes Involved in the Response of *Pyrus betuleafolia* to Drought and High-Temperature Stress. *Plants* **2024**, *13*, 309. <https://doi.org/10.3390/plants13020309>.
23. Ge, M.; Tang, Y.; Guan, Y.; Lv, M.; Zhou, C.; Ma, H.; Lv, J. TaWRKY31, a Novel WRKY Transcription Factor in Wheat, Participates in Regulation of Plant Drought Stress Tolerance. *BMC Plant Biol.* **2024**, *24*, 27. <https://doi.org/10.1186/s12870-023-04709-7>.
24. Luo, D.; Xian, C.; Zhang, W.; Qin, Y.; Li, Q.; Usman, M.; Sun, S.; Xing, Y.; Dong, D. Physiological and Transcriptomic Analyses Reveal Commonalities and Specificities in Wheat in Response to Aluminum and Manganese. *Curr. Issues Mol. Biol.* **2024**, *46*, 367–397. <https://doi.org/10.3390/cimb46010024>.
25. Gonzalez, A.; Brown, M.; Hatlestad, G.; Akhavan, N.; Smith, T.; Hembd, A.; Moore, J.; Montes, D.; Mosley, T.; Resendez, J.; et al. TTG2 Controls the Developmental Regulation of Seed Coat Tannins in Arabidopsis by Regulating Vacuolar Transport Steps in the Proanthocyanidin Pathway. *Dev. Biol.* **2016**, *419*, 54–63. <https://doi.org/10.1016/j.ydbio.2016.03.031>.
26. Jiang, Y.; Liang, G.; Yu, D. Activated Expression of WRKY57 Confers Drought Tolerance in Arabidopsis. *Mol. Plant* **2012**, *5*, 1375–1388. <https://doi.org/10.1093/mp/sss080>.

27. Li, W.; Wang, H.; Yu, D. Arabidopsis WRKY Transcription Factors WRKY12 and WRKY13 Oppositely Regulate Flowering under Short-Day Conditions. *Mol. Plant* **2016**, *9*, 1492–1503. <https://doi.org/10.1016/j.molp.2016.08.003>.
28. Ma, Z.; Li, W.; Wang, H.; Yu, D. WRKY Transcription Factors WRKY12 and WRKY13 Interact with SPL10 to Modulate Age-mediated Flowering. *J. Integr. Plant Biol.* **2020**, *62*, 1659–1673. <https://doi.org/10.1111/jipb.12946>.
29. Chen, W.; Vermaak, I.; Viljoen, A. Camphor—A Fumigant during the Black Death and a Coveted Fragrant Wood in Ancient Egypt and Babylon—A Review. *Molecules* **2013**, *18*, 5434–5454. <https://doi.org/10.3390/molecules18055434>.
30. Zhou, Y.; Yan, W. Conservation and Applications of Camphor Tree (*Cinnamomum camphora*) in China: Ethnobotany and Genetic Resources. *Genet. Resour. Crop Evol.* **2016**, *63*, 1049–1061. <https://doi.org/10.1007/s10722-015-0300-0>.
31. Fazmiya, M.J.A.; Sultana, A.; Rahman, K.; Heyat, M.B. Bin; Sumbul; Akhtar, F.; Khan, S.; Appiah, S.C.Y. Current Insights on Bioactive Molecules, Antioxidant, Anti-Inflammatory, and Other Pharmacological Activities of *Cinnamomum camphora* Linn. *Oxid. Med. Cell. Longev.* **2022**, *2022*, 9354555. <https://doi.org/10.1155/2022/9354555>.
32. Jiang, R.; Chen, X.; Liao, X.; Peng, D.; Han, X.; Zhu, C.; Wang, P.; Hufnagel, D.E.; Wang, L.; Li, K.; et al. A Chromosome-Level Genome of the Camphor Tree and the Underlying Genetic and Climatic Factors for Its Top-Geoherbism. *Front. Plant Sci.* **2022**, *13*, 827890. <https://doi.org/10.3389/fpls.2022.827890>.
33. Lee, S.-H.; Kim, D.-S.; Park, S.-H.; Park, H. Phytochemistry and Applications of *Cinnamomum camphora* Essential Oils. *Molecules* **2022**, *27*, 2695. <https://doi.org/10.3390/molecules27092695>.
34. Li, D.; Lin, H.-Y.; Wang, X.; Bi, B.; Gao, Y.; Shao, L.; Zhang, R.; Liang, Y.; Xia, Y.; Zhao, Y.-P.; et al. Genome and Whole-Genome Resequencing of *Cinnamomum camphora* Elucidate Its Dominance in Subtropical Urban Landscapes. *BMC Biol.* **2023**, *21*, 192. <https://doi.org/10.1186/s12915-023-01692-1>.
35. Wu, Z.; Raven, P.H. (Eds.) *Cinnamomum camphora*. In *Flora of China* 7, 102; Science Press: Beijing, China; Missouri Botanical Garden Press: St. Louis, MO, USA, 2008.
36. Lee, H.J.; Hyun, E.-A.; Yoon, W.J.; Kim, B.H.; Rhee, M.H.; Kang, H.K.; Cho, J.Y.; Yoo, E.S. In Vitro Anti-Inflammatory and Anti-Oxidative Effects of *Cinnamomum camphora* Extracts. *J. Ethnopharmacol.* **2006**, *103*, 208–216. <https://doi.org/10.1016/j.jep.2005.08.009>.
37. Marouf, A.; Harras, F.; Shehata, E.; Abd-Allah, G. Efficacy of Camphor Oil and Its Nano Emulsion on The Cotton Leafworm, *Spodoptera littoralis*. *Egypt. Acad. J. Biol. Sci. F Toxicol. Pest Control* **2021**, *13*, 103–108. <https://doi.org/10.21608/eajbsf.2021.189668>.
38. Zhou, L.; Dong, L.; Huang, Y.; Shi, S.; Zhang, L.; Zhang, X.; Yang, W.; Li, L. Spatial Distribution and Source Apportionment of Polycyclic Aromatic Hydrocarbons (PAHs) in Camphor (*Cinnamomum camphora*) Tree Bark from Southern Jiangsu, China. *Chemosphere* **2014**, *107*, 297–303. <https://doi.org/10.1016/j.chemosphere.2013.12.070>.
39. Zhang, L.; Jing, Z.; Li, Z.; Liu, Y.; Fang, S. Predictive Modeling of Suitable Habitats for *Cinnamomum camphora* (L.) Presl Using Maxent Model under Climate Change in China. *Int. J. Environ. Res. Public Health* **2019**, *16*, 3185. <https://doi.org/10.3390/ijerph16173185>.
40. Xiang, Z.; Zhao, M.; Ogbodo, U.S. Accumulation of Urban Insect Pests in China: 50 Years' Observations on Camphor Tree (*Cinnamomum Camphora*). *Sustainability* **2020**, *12*, 1582. <https://doi.org/10.3390/su12041582>.
41. Yang, Z.; Xie, C.; Huang, Y.; An, W.; Liu, S.; Huang, S.; Zheng, X. Metabolism and Transcriptome Profiling Provides Insight into the Genes and Transcription Factors Involved in Monoterpene Biosynthesis of Borneol Chemotype of *Cinnamomum camphora* Induced by Mechanical Damage. *PeerJ* **2021**, *9*, e11465. <https://doi.org/10.7717/peerj.11465>.
42. Luan, X.; Xu, W.; Zhang, J.; Shen, T.; Chen, C.; Xi, M.; Zhong, Y.; Xu, M. Genome-Scale Identification, Classification, and Expression Profiling of MYB Transcription Factor Genes in *Cinnamomum camphora*. *Int. J. Mol. Sci.* **2022**, *23*, 14279. <https://doi.org/10.3390/ijms232214279>.
43. Lin, H.; Luan, X.; Chen, C.; Gong, X.; Li, X.; Li, H.; Wu, Z.; Liu, Q.; Xu, M.; Zhong, Y. A Systematic Genome-Wide Analysis and Screening of the NAC Family Genes Related to Wood Formation in *Cinnamomum camphora*. *Genomics* **2023**, *115*, 110631. <https://doi.org/10.1016/j.ygeno.2023.110631>.
44. Du, L.; Chen, Z. Identification of Genes Encoding Receptor-like Protein Kinases as Possible Targets of Pathogen- and Salicylic Acid-Induced WRKY DNA-Binding Proteins in Arabidopsis. *Plant J.* **2000**, *24*, 837–847. <https://doi.org/10.1046/j.1365-313x.2000.00923.x>.
45. Dong, J.; Chen, C.; Chen, Z. Expression Profiles of the Arabidopsis WRKY Gene Superfamily during Plant Defense Response. *Plant Mol. Biol.* **2003**, *51*, 21–37. <https://doi.org/10.1023/A:1020780022549>.

46. Yang, Y.; Liu, J.; Zhou, X.; Liu, S.; Zhuang, Y. Identification of WRKY Gene Family and Characterization of Cold Stress-Responsive WRKY Genes in Eggplant. *PeerJ* **2020**, *8*, e8777. <https://doi.org/10.7717/peerj.8777>.
47. Zhang, C.; Wang, D.; Yang, C.; Kong, N.; Shi, Z.; Zhao, P.; Nan, Y.; Nie, T.; Wang, R.; Ma, H.; et al. Genome-Wide Identification of the Potato WRKY Transcription Factor Family. *PLoS ONE* **2017**, *12*, e0181573. <https://doi.org/10.1371/journal.pone.0181573>.
48. Dai, X.; Wang, Y.; Zhang, W.-H. OsWRKY74, a WRKY Transcription Factor, Modulates Tolerance to Phosphate Starvation in Rice. *J. Exp. Bot.* **2016**, *67*, 947–960. <https://doi.org/10.1093/jxb/erv515>.
49. Zhao, Z.; Wang, R.; Su, W.; Sun, T.; Qi, M.; Zhang, X.; Wei, F.; Yu, Z.; Xiao, F.; Yan, L.; et al. A Comprehensive Analysis of the WRKY Family in Soybean and Functional Analysis of GmWRKY164-GmGSL7c in Resistance to Soybean Mosaic Virus. *BMC Genomics* **2024**, *25*, 620. <https://doi.org/10.1186/s12864-024-10523-8>.
50. Guo, X.; Yan, X.; Li, Y. Genome-Wide Identification and Expression Analysis of the WRKY Gene Family in *Rhododendron he-nanense* subsp. *lingbaoense*. *PeerJ* **2024**, *12*, e17435. <https://doi.org/10.7717/peerj.17435>.
51. Yang, J.; Zhang, B.; Gu, G.; Yuan, J.; Shen, S.; Jin, L.; Lin, Z.; Lin, J.; Xie, X. Genome-Wide Identification and Expression Analysis of the R2R3-MYB Gene Family in Tobacco (*Nicotiana Tabacum* L.). *BMC Genom.* **2022**, *23*, 432. <https://doi.org/10.1186/s12864-022-08658-7>.
52. Hu, W.; Ren, Q.; Chen, Y.; Xu, G.; Qian, Y. Genome-Wide Identification and Analysis of WRKY Gene Family in Maize Provide Insights into Regulatory Network in Response to Abiotic Stresses. *BMC Plant Biol.* **2021**, *21*, 427. <https://doi.org/10.1186/s12870-021-03206-z>.
53. Chen, Q.; Fan, D.; Wang, G. Heteromeric Geranyl (Geranyl) Diphosphate Synthase Is Involved in Monoterpene Biosynthesis in Arabidopsis Flowers. *Mol. Plant* **2015**, *8*, 1434–1437. <https://doi.org/10.1016/j.molp.2015.05.001>.
54. Qin, W.; Wang, N.; Yin, Q.; Li, H.; Wu, A.-M.; Qin, G. Activation Tagging Identifies WRKY14 as a Repressor of Plant Thermomorphogenesis in Arabidopsis. *Mol. Plant* **2022**, *15*, 1725–1743. <https://doi.org/10.1016/j.molp.2022.09.018>.
55. Hou, J.; Zhang, J.; Zhang, B.; Jin, X.; Zhang, H.; Jin, Z. Transcriptional Analysis of Metabolic Pathways and Regulatory Mechanisms of Essential Oil Biosynthesis in the Leaves of *Cinnamomum Camphora* (L.) Presl. *Front. Genet.* **2020**, *11*, 598714. <https://doi.org/10.3389/fgene.2020.598714>.
56. Zhang, T.; Zheng, Y.; Fu, C.; Yang, H.; Liu, X.; Qiu, F.; Wang, X.; Wang, Z. Chemical Variation and Environmental Influence on Essential Oil of *Cinnamomum camphora*. *Molecules* **2023**, *28*, 973. <https://doi.org/10.3390/molecules28030973>.
57. Chen, G.; Mostafa, S.; Lu, Z.; Du, R.; Cui, J.; Wang, Y.; Liao, Q.; Lu, J.; Mao, X.; Chang, B.; et al. The Jasmine (*Jasminum sambac*) Genome Provides Insight into the Biosynthesis of Flower Fragrances and Jasmonates. *Genom. Proteom. Bioinform.* **2023**, *21*, 127–149. <https://doi.org/10.1016/j.gpb.2022.12.005>.
58. Zhao, Q.; Zhong, X.-L.; Zhu, S.-H.; Wang, K.; Tan, G.-F.; Meng, P.-H.; Zhang, J. Research Advances in Toona Sinensis, a Traditional Chinese Medicinal Plant and Popular Vegetable in China. *Diversity* **2022**, *14*, 572. <https://doi.org/10.3390/d14070572>.
59. Wu, L.; Liu, J.; Huang, W.; Wang, Y.; Chen, Q.; Lu, B. Exploration of Osmanthus Fragrans Lour.’s Composition, Nutraceutical Functions and Applications. *Food Chem.* **2022**, *377*, 131853. <https://doi.org/10.1016/j.foodchem.2021.131853>.
60. Dudareva, N.; Pichersky, E. Biochemical and Molecular Genetic Aspects of Floral Scents. *Plant Physiol.* **2000**, *122*, 627–634. <https://doi.org/10.1104/pp.122.3.627>.
61. Dudareva, N.; Klempien, A.; Muhlemann, J.K.; Kaplan, I. Biosynthesis, Function and Metabolic Engineering of Plant Volatile Organic Compounds. *New Phytol.* **2013**, *198*, 16–32. <https://doi.org/10.1111/nph.12145>.
62. Abbas, F.; Ke, Y.; Yu, R.; Yue, Y.; Amanullah, S.; Jahangir, M.M.; Fan, Y. Volatile Terpenoids: Multiple Functions, Biosynthesis, Modulation and Manipulation by Genetic Engineering. *Planta* **2017**, *246*, 803–816. <https://doi.org/10.1007/s00425-017-2749-x>.
63. Ding, W.; Ouyang, Q.; Li, Y.; Shi, T.; Li, L.; Yang, X.; Ji, K.; Wang, L.; Yue, Y. Genome-Wide Investigation of WRKY Transcription Factors in Sweet Osmanthus and Their Potential Regulation of Aroma Synthesis. *Tree Physiol.* **2020**, *40*, 557–572. <https://doi.org/10.1093/treephys/tpz129>.
64. Lu, Z.; Wang, X.; Mostafa, S.; Noor, I.; Lin, X.; Ren, S.; Cui, J.; Jin, B. WRKY Transcription Factors in *Jasminum sambac*: An Insight into the Regulation of Aroma Synthesis. *Biomolecules* **2023**, *13*, 1679. <https://doi.org/10.3390/biom13121679>.
65. Ren, L.; Wan, W.; Yin, D.; Deng, X.; Ma, Z.; Gao, T.; Cao, X. Genome-Wide Analysis of WRKY Transcription Factor Genes in *Toona sinensis*: An Insight into Evolutionary Characteristics and Terpene Synthesis. *Front. Plant Sci.* **2023**, *13*, 1063850. <https://doi.org/10.3389/fpls.2022.1063850>.

66. Yu, Y.; Lyu, S.; Chen, D.; Lin, Y.; Chen, J.; Chen, G.; Ye, N. Volatiles Emitted at Different Flowering Stages of *Jasminum sambac* and Expression of Genes Related to α -Farnesene Biosynthesis. *Molecules* **2017**, *22*, 546. <https://doi.org/10.3390/molecules22040546>.
67. Barman, M.; Mitra, A. Temporal Relationship between Emitted and Endogenous Floral Scent Volatiles in Summer- and Winter-blooming *Jasminum* Species. *Physiol. Plant.* **2019**, *166*, 946–959. <https://doi.org/10.1111/ppl.12849>.
68. Johnson, C.S.; Kolevski, B.; Smyth, D.R. TRANSPARENT TESTA GLABRA2, a Trichome and Seed Coat Development Gene of *Arabidopsis*, Encodes a WRKY Transcription Factor. *Plant Cell* **2002**, *14*, 1359–1375. <https://doi.org/10.1105/tpc.001404>.
69. Guo, D.; Zhang, J.; Wang, X.; Han, X.; Wei, B.; Wang, J.; Li, B.; Yu, H.; Huang, Q.; Gu, H.; et al. The WRKY Transcription Factor WRKY71/EXB1 Controls Shoot Branching by Transcriptionally Regulating RAX Genes in *Arabidopsis*. *Plant Cell* **2015**, *27*, 3112–3127. <https://doi.org/10.1105/tpc.15.00829>.
70. Mistry, J.; Chuguransky, S.; Williams, L.; Qureshi, M.; Salazar, G.A.; Sonnhammer, E.L.L.; Tosatto, S.C.E.; Paladin, L.; Raj, S.; Richardson, L.J.; et al. Pfam: The Protein Families Database in 2021. *Nucleic Acids Res.* **2021**, *49*, D412–D419. <https://doi.org/10.1093/nar/gkaa913>.
71. Chen, C.; Wu, Y.; Li, J.; Wang, X.; Zeng, Z.; Xu, J.; Liu, Y.; Feng, J.; Chen, H.; He, Y.; et al. TBtools-II: A “One for All, All for One” Bioinformatics Platform for Biological Big-Data Mining. *Mol. Plant* **2023**, *16*, 1733–1742. <https://doi.org/10.1016/j.molp.2023.09.010>.
72. Wang, J.; Chitsaz, F.; Derbyshire, M.K.; Gonzales, N.R.; Gwadz, M.; Lu, S.; Marchler, G.H.; Song, J.S.; Thanki, N.; Yamashita, R.A.; et al. The Conserved Domain Database in 2023. *Nucleic Acids Res.* **2023**, *51*, D384–D388. <https://doi.org/10.1093/nar/gkac1096>.
73. Gasteiger, E.; Hoogland, C.; Gattiker, A.; Duvaud, S.; Wilkins, M.R.; Appel, R.D.; Bairoch, A. Protein Identification and Analysis Tools on the ExPASy Server. In *The Proteomics Protocols Handbook*; Humana Press: Totowa, NJ, USA, 2005; pp. 571–607.
74. Horton, P.; Park, K.-J.; Obayashi, T.; Fujita, N.; Harada, H.; Adams-Collier, C.J.; Nakai, K. WoLF PSORT: Protein Localization Predictor. *Nucleic Acids Res.* **2007**, *35*, W585–W587. <https://doi.org/10.1093/nar/gkm259>.
75. Almagro Armenteros, J.J.; Salvatore, M.; Emanuelsson, O.; Winther, O.; von Heijne, G.; Elofsson, A.; Nielsen, H. Detecting Sequence Signals in Targeting Peptides Using Deep Learning. *Life Sci. Alliance* **2019**, *2*, e201900429. <https://doi.org/10.26508/lsa.201900429>.
76. Nguyen Ba, A.N.; Pogoutse, A.; Provar, N.; Moses, A.M. NLStradamus: A Simple Hidden Markov Model for Nuclear Localization Signal Prediction. *BMC Bioinform.* **2009**, *10*, 202. <https://doi.org/10.1186/1471-2105-10-202>.
77. R Core Team. *R: A Language and Environment for Statistical Computing*; R Foundation for Statistical Computing: Vienna, Austria, 2021.
78. Katoh, K.; Standley, D.M. MAFFT Multiple Sequence Alignment Software Version 7: Improvements in Performance and Usability. *Mol. Biol. Evol.* **2013**, *30*, 772–780. <https://doi.org/10.1093/molbev/mst010>.
79. Capella-Gutiérrez, S.; Silla-Martínez, J.M.; Gabaldón, T. TrimAl: A Tool for Automated Alignment Trimming in Large-Scale Phylogenetic Analyses. *Bioinformatics* **2009**, *25*, 1972–1973. <https://doi.org/10.1093/bioinformatics/btp348>.
80. Hoang, D.T.; Chernomor, O.; von Haeseler, A.; Minh, B.Q.; Vinh, L.S. UFBoot2: Improving the Ultrafast Bootstrap Approximation. *Mol. Biol. Evol.* **2018**, *35*, 518–522. <https://doi.org/10.1093/molbev/msx281>.
81. Minh, B.Q.; Schmidt, H.A.; Chernomor, O.; Schrempf, D.; Woodhams, M.D.; von Haeseler, A.; Lanfear, R. IQ-TREE 2: New Models and Efficient Methods for Phylogenetic Inference in the Genomic Era. *Mol. Biol. Evol.* **2020**, *37*, 1530–1534. <https://doi.org/10.1093/molbev/msaa015>.
82. Kalyaanamoorthy, S.; Minh, B.Q.; Wong, T.K.F.; von Haeseler, A.; Jermini, L.S. ModelFinder: Fast Model Selection for Accurate Phylogenetic Estimates. *Nat. Methods* **2017**, *14*, 587–589. <https://doi.org/10.1038/nmeth.4285>.
83. Xie, J.; Chen, Y.; Cai, G.; Cai, R.; Hu, Z.; Wang, H. Tree Visualization By One Table (TvBOT): A Web Application for Visualizing, Modifying and Annotating Phylogenetic Trees. *Nucleic Acids Res.* **2023**, *51*, W587–W592. <https://doi.org/10.1093/nar/gkad359>.
84. Crooks, G.E.; Hon, G.; Chandonia, J.-M.; Brenner, S.E. WebLogo: A Sequence Logo Generator. *Genome Res.* **2004**, *14*, 1188–1190. <https://doi.org/10.1101/gr.849004>.
85. Waterhouse, A.M.; Procter, J.B.; Martin, D.M.A.; Clamp, M.; Barton, G.J. Jalview Version 2—A Multiple Sequence Alignment Editor and Analysis Workbench. *Bioinformatics* **2009**, *25*, 1189–1191. <https://doi.org/10.1093/bioinformatics/btp033>.

86. Madeira, F.; Madhusoodanan, N.; Lee, J.; Eusebi, A.; Niewielska, A.; Tivey, A.R.N.; Lopez, R.; Butcher, S. The EMBL-EBI Job Dispatcher Sequence Analysis Tools Framework in 2024. *Nucleic Acids Res.* **2024**, *52*, W521–W525. <https://doi.org/10.1093/nar/gkae241>.
87. Tamura, K.; Stecher, G.; Kumar, S. MEGA11: Molecular Evolutionary Genetics Analysis Version 11. *Mol. Biol. Evol.* **2021**, *38*, 3022–3027. <https://doi.org/10.1093/molbev/msab120>.
88. Bailey, T.L.; Johnson, J.; Grant, C.E.; Noble, W.S. The MEME Suite. *Nucleic Acids Res.* **2015**, *43*, W39–W49. <https://doi.org/10.1093/nar/gkv416>.
89. Lescot, M. PlantCARE, a Database of Plant Cis-Acting Regulatory Elements and a Portal to Tools for in Silico Analysis of Promoter Sequences. *Nucleic Acids Res.* **2002**, *30*, 325–327. <https://doi.org/10.1093/nar/30.1.325>.
90. Schroeder, A.; Mueller, O.; Stocker, S.; Salowsky, R.; Leiber, M.; Gassmann, M.; Lightfoot, S.; Menzel, W.; Granzow, M.; Ragg, T. The RIN: An RNA Integrity Number for Assigning Integrity Values to RNA Measurements. *BMC Mol. Biol.* **2006**, *7*, 3. <https://doi.org/10.1186/1471-2199-7-3>.
91. Kim, D.; Paggi, J.M.; Park, C.; Bennett, C.; Salzberg, S.L. Graph-Based Genome Alignment and Genotyping with HISAT2 and HISAT-Genotype. *Nat. Biotechnol.* **2019**, *37*, 907–915. <https://doi.org/10.1038/s41587-019-0201-4>.
92. Pertea, M.; Kim, D.; Pertea, G.M.; Leek, J.T.; Salzberg, S.L. Transcript-Level Expression Analysis of RNA-Seq Experiments with HISAT, StringTie and Ballgown. *Nat. Protoc.* **2016**, *11*, 1650–1667. <https://doi.org/10.1038/nprot.2016.095>.
93. Love, M.I.; Huber, W.; Anders, S. Moderated Estimation of Fold Change and Dispersion for RNA-Seq Data with DESeq2. *Genome Biol.* **2014**, *15*, 550. <https://doi.org/10.1186/s13059-014-0550-8>.
94. Bu, D.; Luo, H.; Huo, P.; Wang, Z.; Zhang, S.; He, Z.; Wu, Y.; Zhao, L.; Liu, J.; Guo, J.; et al. KOBAS-i: Intelligent Prioritization and Exploratory Visualization of Biological Functions for Gene Enrichment Analysis. *Nucleic Acids Res.* **2021**, *49*, W317–W325. <https://doi.org/10.1093/nar/gkab447>.
95. Wong, M.L.; Medrano, J.F. Real-Time PCR for mRNA Quantitation. *Biotechniques* **2005**, *39*, 75–85. <https://doi.org/10.2144/05391RV01>.
96. Koressaar, T.; Remm, M. Enhancements and Modifications of Primer Design Program Primer3. *Bioinformatics* **2007**, *23*, 1289–1291. <https://doi.org/10.1093/bioinformatics/btm091>.
97. Livak, K.J.; Schmittgen, T.D. Analysis of Relative Gene Expression Data Using Real-Time Quantitative PCR and the $2^{-\Delta\Delta CT}$ Method. *Methods* **2001**, *25*, 402–408. <https://doi.org/10.1006/meth.2001.1262>.

Disclaimer/Publisher’s Note: The statements, opinions and data contained in all publications are solely those of the individual author(s) and contributor(s) and not of MDPI and/or the editor(s). MDPI and/or the editor(s) disclaim responsibility for any injury to people or property resulting from any ideas, methods, instructions or products referred to in the content.